MDPI

Article

Effect of Oily Aerosol Charge Characteristics on the Filtration Efficiency of an Electrostatically Enhanced Fibrous Filter System

Yi Yu, Di Pan, Kai Kang, Shu-Pei Bai, Hao Han, Hua Song * and Jian Kang *

State Key Laboratory of NBC Protection for Civilian, Beijing 102205, China
* Correspondence: songhua@sklnbcpc.cn (H.S.); larance0130@163.com (J.K.)

Abstract: The synergistic effect of electrostatically enhanced fibrous filtration originates from the charging characteristics of aerosol particles and electret fibers in an electric field. Two electrostatically enhanced fibrous filter systems are designed in this study to investigate the mechanism of the effects of the charging characteristics of oily aerosol on the filtration efficiency. We investigate the charging characteristics and their effects on the filtration efficiency of dioctyl-phthalate (DOP) aerosol particles of various sizes by setting different filter systems and electric field intensities. The experimental results show that the charge of DOP particles increases with the strength of the electric field, and the average charge increases with the particle size. The maximum charge of DOP particles reaches 4760 eC/P, and the filtration efficiency of the coupled system improves when DOP particles are amply charged. For 0.25 μm DOP particles as the most penetrating particle size, the system had good long-term stability, and the filtration efficiency is approximately 72% higher than that of the fiber acting alone. Meanwhile, the problem of oily aerosol deposition reducing the electret filtration efficiency is solved, providing a basis for long-term filtration and oily aerosol purification by electret fiber.

Keywords: electric field enhancement; air filtration; dioctyl- phthalate aerosol; charge

1. Introduction

Concerns relating to air pollution and public health, especially the ongoing pandemic of novel coronavirus pneumonia (COVID-19), have increased the demand for and attention to the treatment of aerosol pollution in recent decades [1–4]. Electrostatic precipitator technology and fiber filtration technology are the gas-cleaning technologies most commonly used for the removal of aerosol particles in atmospheric filtration [5,6]. Electrostatic precipitator technology charges particles with a high-voltage electric field such that they move in a certain direction and are collected by a dust-collecting plate. However, the electrostatic precipitator technology poorly filters ultrafine particles and generates ozone (O_3) and other by-products [5,7]. Fiber filtration technology uses mechanical means of capturing particles, such as direct interception and inertial sedimentation. However, it faces the problem of high pressure in the efficient filtering of fine particles [8–10].

Electrostatically enhanced fibrous filtration technology takes advantage of both electrostatic filtration technology and fiber filtration technology. Relevant equipment not only effectively collects submicron fine particles but also has a low resistance, a long service life, and low energy consumption and is thus suited to the filtration of aerosols [11–13]. This technology is widely used to purify cooking oil fume and oily aerosol produced by machining processes, ship engines, and diesel-powered vehicles [14–17]. In the electrostatically enhanced fibrous filter system, there is air ionization around the electrode to produce O_3 because of the application of a high voltage, so the ozone concentration should be monitored in case of causing secondary pollution [18–21].

According to Coulomb's law, the electrostatic force increases with the charge of an aerosol [22,23]. For both the electrostatic precipitator technology and the electrostatically enhanced fibrous filtration technology, the Coulomb force generated by the charging of

aerosol particles greatly affects the filtration process. In the electrostatically enhanced fibrous filtration process, the charging characteristics of aerosol relate to the filtration efficiency [24]. The charge of aerosol particles also affects the sedimentation form of the aerosols [25,26]. The form and intensity of the electric field were the main factors affecting the purification efficiency in a study of the effect of the electric field on the filtration efficiency of an oily aerosol [27,28]. This also applies to bioaerosols. Xu et al. [29] used an electrostatic precipitator with parallel plates to charge microbial aerosols, finding that a stronger electric field improved the charge and collection efficiency of the bioaerosols. Wang et al. [30] showed that the influence of electrostatic force on charged dust aerosol was related to the charge of the dust layer and particles in the electrostatic fabric filter. An increase in voltage improved the filtration efficiency owing to a greater disorder of the movement of charged particles, resulting in full diffusion in the precipitator.

The mechanism of enhanced filtration efficiency by an electrostatically enhanced fibrous filter system is very complex and is affected by fiber charging, aerosol charging, and electric field. Studying the charge law of aerosols can enhance the understanding of the collaborative filtering mechanisms from one side. However, most studies on aerosol charging have focused on solid aerosols, and the relationship between the charging characteristics of oily aerosols and enhanced filtration efficiency requires further research. Additionally, there have been few reports on the charge amount of aerosol in an electric field. In relevant equipment, the electric field is arranged in various forms to increase the charging effect, improve filtration efficiency, and reduce the pressure drop [31–33]. The present paper thus investigates the factors affecting the filtration efficiency of oil-based aerosols for two self-designed electrostatically enhanced fibrous filter systems. The paper further analyzes the charging of DOP aerosols and the filtering performance of the two coupled systems. The purpose of this study was to analyze the influencing factors on oily aerosol charging and the effect of charging characteristics on the filtering performance of the coupled system. These factors were the form of the electric field and the electric field intensity. This study can provide a reference for the structural design and setting of the engineering parameters for the electrostatically enhanced fibrous filter system.

2. Materials and Methods

2.1. Experimental System

As shown in Figure 1a, the electrostatically enhanced fibrous filter experimental system had three main parts for aerosol generation, aerosol charging, and data collection, and analysis. The experimental air duct was made from polymethyl methacrylate and had a square cross-section of 200 mm × 200 mm and a total length of 3.5 m. The air duct was divided into two sections, namely, an upstream section having a length of 1500 mm and a downstream section having a length of 2000 mm. In the air duct, a flange connection was set in the middle to connect the aerosol charging reactor and filter material. A sampling port was set in each of the upper section and downstream sections to monitor the face velocity, particle size distribution, quantity concentration, and charge amount of the DOP aerosol. The experimental air volume was controlled to be 14.4 ± 0.1 m^3/h by a variable-frequency fan and vortex flowmeter at the end of the air duct. The high voltage range of high voltage DC power supply (Dongwen, Tianjin, China) was 0–50 kV for negative polarity. The accuracy was 0.01 kV. The ozone concentration of coupled systems was measured by the photometric ozone analyzer (106-L, 2B-Technologies, Boulder, CO, USA). The measuring range was 0–500 ppb and the accuracy was 0.1 ppb. The sampling port was set in the downstream section of air duct to monitor the ozone concentration. The distance between air duct opening and sampling port was 10 cm. The discharged current was measured by the ammeter (ZGF-Z2, Guodianzhongxing, Wuhan, China) in different experimental conditions. The measuring range was 0–2 mA, and its accuracy was 1 μA.
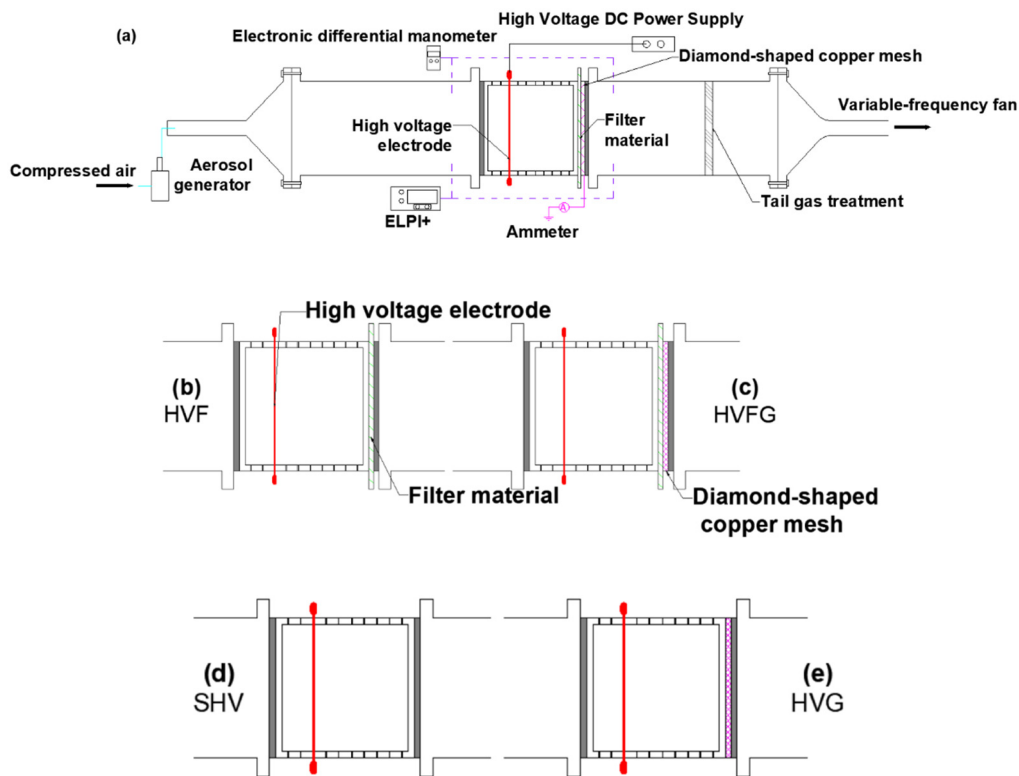
Figure 1. Experimental setup for electrostatically enhanced fibrous filter system (**a**) schematic diagram of the experimental system (**b**) schematic diagram of the HVF (**c**) schematic diagram of the HVFG (**d**) schematic diagram of the SHV (**e**) schematic diagram of the HVG.

2.1.1. Aerosol Generation

DOP was used as the medium to generate oily aerosol. Compressed air was passed through an organic aerosol generator (Agf10.0, Palas, Karlsruhe, Germany) to produce oily aerosol, which was mixed with a large amount of air in the mixing section at the inlet of the experimental pipeline. The mixture became stable and uniform after mixing and rectifying through the upstream pipeline. The aerosol concentration was varied by adjusting the gas flow of the aerosol generator. The total aerosol concentration in the experiment was 10^5 P/cm^3, and the particle size measured using an Electrical Low-Pressure Impactor (ELPI$^+$) was 0.03–3.68 μm (median size of approximately 0.4 μm). The particle size distribution is shown in Figure 2.

2.1.2. Aerosol Charging

The part of aerosol charging was mainly formed by the aerosol charging reactor, filter material, and diamond-shaped copper mesh. Wire electrodes were installed in the aerosol charging reactor, and the installation location could be changed to adjust the distance between copper wires and the grounding electrode. As shown in Figure 1b,c in this study, we designed two coupled systems, namely, a 'high voltage electrode-fiber-grounding electrode' coupled system (HVFG) and a 'high voltage electrode-fiber' coupled system (HVF), with the difference being that the former had a special device for the grounding electrode. The HVFG was composed of high-voltage wire electrodes, filter material, and the grounding electrode, and it was similar to an electrostatic precipitator coupled with filter material. The HVF was formed by high-voltage wire electrodes and filter material, and the filter material was installed downstream of wire electrodes, so it could be seen as an ionizing coupled with filtration. When the filter material was removed from above two systems, the HVFG changed to the 'high voltage electrode–grounding electrode' system (HVG), while the HVF changed to the 'suspended high-voltage electrodes' (SHV). The configuration of SHV is shown in Figure 1d. The SHV was only formed by wire electrodes,

so it was similar to an ionizing device. As shown in Figure 1e, the HVG was an ESP device with the structure of wire electrodes and a grounding electrode.
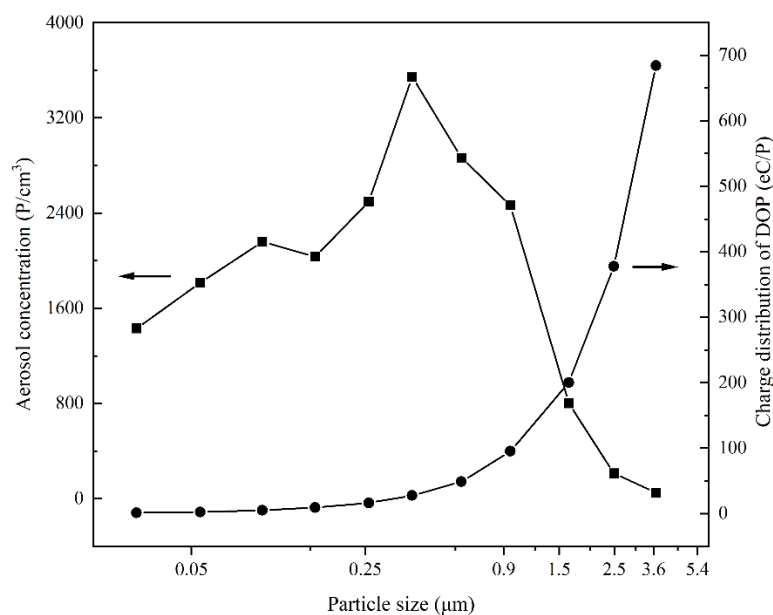
Figure 2. Particle size distribution and charge distribution of DOP measured by the ELPI$^+$.

The high-voltage wire electrodes were five copper wires, each with a diameter of 0.2 mm and a length of 200 mm. These copper wires were evenly arranged in the air duct perpendicular to the direction of airflow. The grounding electrode was a diamond-shaped copper mesh with a side length of 8 mm, placed parallel to the high-voltage electrode wire. The metal grid of diamond-shaped copper mesh was composed of copper wires with a net wire diameter of 1 mm, and the distance between two copper wires was 2.7 mm. The thickness of this diamond-shaped copper mesh was 1 mm. The filter material was polypropylene fiber with an areal fiber weight of 22 g/m^3 (PP22 g). The electric field intensity was varied by adjusting the distance between the line electrode and grounding electrode or the output voltage of the high-voltage direct current (DC) power supply.

Considering that the electric field generated by the wire electrode and grounding electrode was uneven, the electric field intensity was varied by fixing the applied voltage but adjusting the distance between the wire electrode and grounding electrode or by fixing the distance between the electrodes but adjusting the applied voltage. The HVF was composed of high-voltage electrodes and filter materials. The electric field of the HVF was generated by suspended high-voltage electrodes (SHV). The electric field intensity was varied by adjusting the distance between the wire electrode and the air duct outlet downstream of the aerosol charging section where the filter material was placed. The grounding electrode was placed in the air duct opening of this section, and thus, for the same initial distance of two types of electrodes, the operation of varying the electric field intensity by adjusting the distance had the same effect in the two systems.

2.1.3. Data Acquisition and Analysis

Data on the charging characteristics were obtained using an ELPI$^+$ (Dekati, Kangasala, Finland). The aerosol concentration with long-term stability was measured by an aerosol spectrometer (Promo 2000, Palas, Karlsruhe, Germany). The particle size distribution, number concentration, and charge amount were obtained before and after the charging of the aerosol by switching the sampling ports of the upstream and downstream air ducts of the experimental pipeline.

2.2. Experimental Methodology

2.2.1. Method of Determining the Aerosol Charge

In accordance with the measurement principle of the ELPI$^+$, the particle size distribution and charge amount of the aerosol were monitored in real-time by turning on or off the charging switch of the ELPI$^+$. The main principle is that the charged aerosol has inertia to pass through a certain number of 14 low-pressure cascade impactors, with each impactor connecting to a sensitive electrometer that measures the induced current of particles passing through that impactor stage. This current is directly proportional to the number concentration of particles in the stage. When the charging switch of the ELPI$^+$ is turned on, the collected aerosol is charged to a known level in a positive corona charger. After their collection, the particles are classified by their aerodynamic particle size in a low-pressure cascade impactor, and the aerosol concentration of each impactor stage (i.e., each particle size segment) is then measured. The ELPI$^+$ used in the experiment measured particles in 14 size fractions ranging from 6 nm to 10 μm. When the charge switch of the ELPI$^+$ is turned off, the ELPI$^+$ measures the charge distribution of the charged aerosol.

The induced current of each impactor stage reflects the total current of all particles within the particle size range. The relationship between the average charge of aerosol and the induced current is thus

$$Q_i = \frac{|I_i|}{V \times C_i} \tag{1}$$

where I_i is the induced current of stage i measured by the sensitive electrometers (A); C_i is the DOP quantity concentration of level i measured by the ELPI$^+$ (P/cm^3); V is the sampling flow (cm^3/s); Q_i is the average charge of a single aerosol particle in the level i particle size section of DOP (eC/P).

For the DOP aerosol used in this experiment, in accordance with the measurement principle of the ELPI$^+$, the charge distribution of DOP measured by the ELPI$^+$ in each particle size class is calculated as shown in Figure 2.

2.2.2. Model of the Particle Filtration Efficiency

There are two states of the electrostatically enhanced fibrous filter system, namely, the on and off states of the negative high-voltage DC power supply. Therefore, the fractional concentration of DOP aerosol can be tested at symmetrical positions of the upstream and downstream air channels of the aerosol charger. The fractional efficiency of the oily DOP aerosol within the particle size range of level j is calculated as

$$\eta_j = \frac{C_{jin} - C_{jout}}{C_{jin}} \times 100\%, \tag{2}$$

where C_{jin} and C_{jout} are respectively the quantity concentrations of the level j particle size range of aerosol measured upstream and downstream of the electrostatically enhanced fibrous filter system (P/cm^3).

3. Results

3.1. Filtering Performances of the Two Coupled Systems

The enhancement effects of the HVFG and HVF on the filtration efficiency are shown in Figure 3. The results show that the two coupled systems had effectively improved the filtering effects of the filter material under the same experimental conditions of the air volume and DOP concentration. At a negative voltage of −30 kV, the filtration efficiency for DOP charged in the electric field generated by the SHV was low. The fractional efficiency gradually increased with the DOP particle size at a small particle size, whereas it was basically stable at approximately 25% for DOP particles larger than 0.25 μm. In the case of the HVF, there was a downward trend in the fractional efficiency in the particle size range of 0.15–0.25 μm when the filter material acted alone at the same voltage. The filtration efficiency of the coupled system improved by approximately 10% for DOP aerosol having a

particle size smaller than 0.38 µm, and the improvement gradually decreased as the particle size increased beyond 0.38 µm.
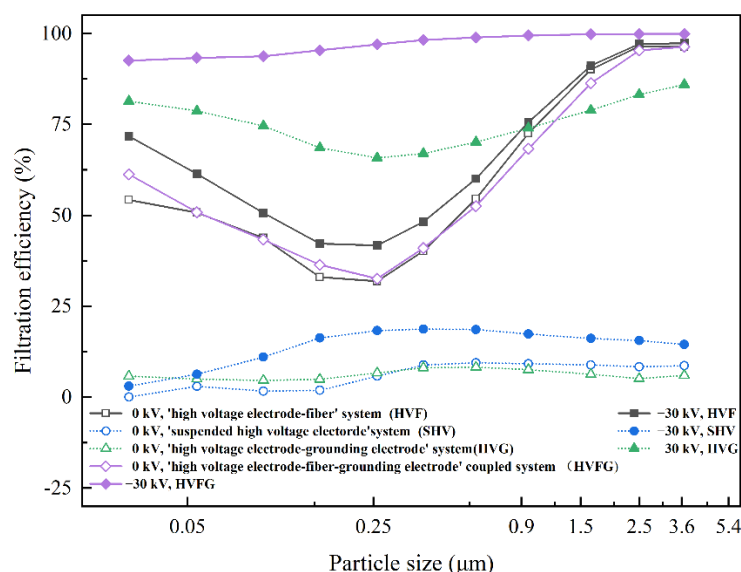
Figure 3. Effects of coupled forms on the filtration efficiency.

Figure 3 also shows that, at the same voltage, the filtration efficiency of HVG for DOP having a particle size of 0.25 µm reached 65.8%, which was much higher than the electrode discharge of 18.3% in the suspended state. Additionally, at an applied voltage of −30 kV, the HVFG had a high filtration efficiency for each particle size, i.e., the filtration efficiency was approximately 92% for the smallest particles and reached 97% for particles larger than 0.25 µm. Furthermore, the filtration efficiency of the coupled system increased with the DOP particle size, but there was no penetration particle size ranging from 0.15 to 0.25 µm. The electrostatically enhanced fibrous filter system thus overcomes the problem of the most penetrating particle size in single filtration technology.

3.2. DOP Charging Effects of the Coupled Systems

Theoretical analysis of the electrostatically enhanced fibrous filter has shown that the main reason for the enhanced filtration efficiency is that the precharging of aerosol particles by the electric field increases the Coulomb force of the aerosol particles passing through the filter material. The present study investigated the charging of DOP oil aerosol in an electric field and its effects on the filtration efficiency of the coupled system.

The charging characteristics of DOP in the two coupled systems are shown in Figure 4. Figure 4a shows that when the system did not have a special device for the grounding electrode, the charging of DOP aerosol by the HVF was poor. When the applied negative voltage was lower than −30 kV, the charge of the aerosol did not increase appreciably, and the charge of the DOP particles was far less than the ample charge of the ELPI⁺. This is because the SHV generates a weak corona discharge when high pressure is applied, and the aerosol is thus charged by ions generated by ionized air. There is no specific device grounded, and the increase in the applied voltage thus does not appreciably improve the coronal discharge effect. The concentration of negative ions generated in the air is low, which reduces the probability of combining with particles and leads to the poor charging of DOP aerosol. Figure 4b presents the DOP aerosol charge for the grounding system. It is seen that for the electric field of the coupled system with a specific grounded device behind the wire electrode, the applied voltage remarkably affects the aerosol charge. When the negative voltage was stronger than −20 kV, the electric field generated by the wire electrodes and grounding electrode better charged the DOP aerosol than did the ELPI⁺. The charge amount of aerosol increased continuously with the applied voltage; the charge

of particles smaller than 1.5 µm increased slowly, whereas that of larger particles changed more rapidly.
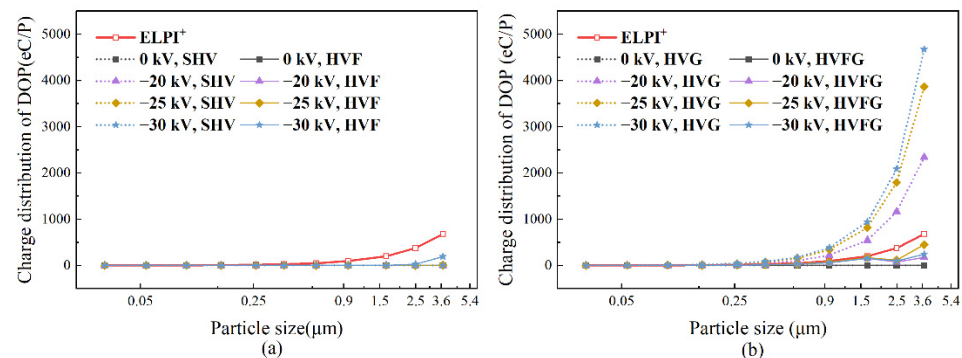
Figure 4. Effects of coupled forms on DOP charging. (**a**) Charge distribution of DOP for the system without a grounding electrode. (**b**) Charge distribution of DOP for the grounding system.

The results of the filtration efficiency of the system presented in Figure 3 show that the improvement in the filtration efficiency of the coupled system due to the charging by the electric field well matches the charging effect in the electric field. Under the same conditions, the improvement in DOP charging due to the SHV discharge was far less than that due to electric field discharge with the grounding electrode. For the same high DC voltage of −30 kV, the average charge of DOP aerosol particles with a size of 3.68 µm was 191.8 eC/P after the particles passed through the electric field generated by the SHV, whereas the charge was 24.4 times as large for the HVG. The results show that the aerosol charge affected the filtration efficiency of the coupled system. Under the above conditions, the filtration efficiency was only 18.3% when there was no grounding electrode and 65.8% when there was a grounding electrode for the DOP particles, with the most penetrating particle size being 0.25 µm for the electric field and filter material. In the coupled system of the electric field and filter material, the charged DOP particles are more likely to be intercepted and captured by the filter material because of the action of the Coulomb force. There is an upper limit for the effect of the Coulomb force, and the difference in the effect of the aerosol charge on the filtration efficiency of the coupled system is thus due to the presence of a sufficient charge. The filtration efficiency is better when the average charge is higher than the stable charge of the ELPI$^+$ for DOP charging. In the example of a particle size of 0.25 µm, the filtration efficiency was 43% for the HVF and 96.6% for the HVFG. Additionally, for the coupled system with filter material, the filtration efficiency improved, and the charge of DOP particles was reduced after filtering with the filter material, indicating that the improvement in the filtration efficiency of the coupled system was mainly due to the charged particles strengthening the Coulomb force. The probability that DOP particles passing through the filter material were intercepted and filtered by the filter material was increased.

3.3. Effect of the Electric Field Intensity on the Filtering Effects of the Coupled Systems

The effects of factors such as the electric field intensity on the DOP charge and corresponding filtration efficiency in the HVFG are further studied to clarify the mechanism of the enhancement effect of the DOP charge on the filtration efficiency in the electrostatically enhanced fibrous filter system. The electric field intensity is the main factor that affects the aerosol charge and can be varied by adjusting the voltage or the distance between the two types of electrodes.

The V-I relationship of the coupled system with and without the filter material was measured when the coupled system had a grounding electrode. Figure 5 shows the V-I characteristics of the HVG and HVFG. Additionally, the V-I relationship was also changed because of the adjustment of voltage or the distance between the two types of electrodes. At

the same distance between the wires electrodes and grounding electrode, the current value increased with the increase in voltage for the two coupled systems. At the same voltage, the current value decreased as the above distance increased for two coupled systems.
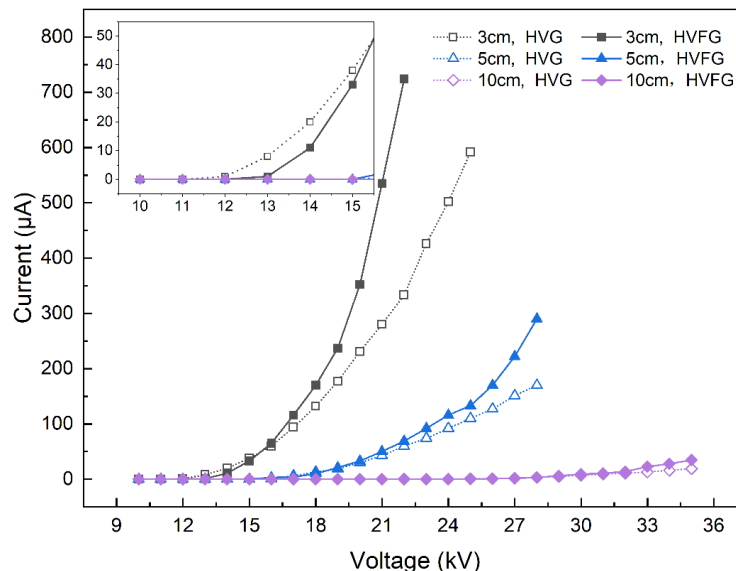

Figure 5. The voltage-current relationship of the HVG and HVFG.

We first fixed the voltage and adjusted the distance between the wire electrode and grounding electrode to analyze the effects of the electric field intensity on the DOP charge and the filtration efficiency of the HVFG. With the applied voltage fixed at -20 kV, the electric field intensity was varied by adjusting the separation of the two electrodes between 3 and 10 cm. The charge of DOP aerosol particles and the filtration efficiency of the coupled system at different electric field intensities are shown in Figure 6.

Figure 6a shows that for the electric field generated by the wire electrode and grounding electrode, the charge of the DOP aerosol increased with the electric field intensity, and for DOP aerosol particles larger than 1 μm, the charge of a single particle increased with the particle size. This is because the electric field of the 'high voltage electrode–grounding electrode' structure was non-uniform. When a high negative DC voltage is applied, the wire electrode creates a corona discharge and a region of ionization forms around the discharge electrode [34–36]. The gas molecules are ionized and release a large number of free electrons, forming a Trichel pulse [37–39]. As the electric field strengthens, an electron avalanche forms, which intensifies the ionization of gas molecules. The ionization reaction continues to generate many electrons, thus improving the spatial charge density and the charging of the aerosol improves [40–42]. At the same time, because the particle size of aerosols affects the charge of the particles in the electric field, the average charge of particles increases with the particle size under the two charging mechanisms of diffusion and collision. However, aerosol particles smaller than 1 μm have a low charge capacity. Even if the number concentration is high, the effect of the field strength on the charge is not obvious, and the charge of small aerosol particles readily reaches a balance. The charge capacity increases appreciably for aerosol particles larger than 1 μm, which explains how the charge of particles larger than 1 μm increases appreciably with the field strength [24,30].

(a)

(b)
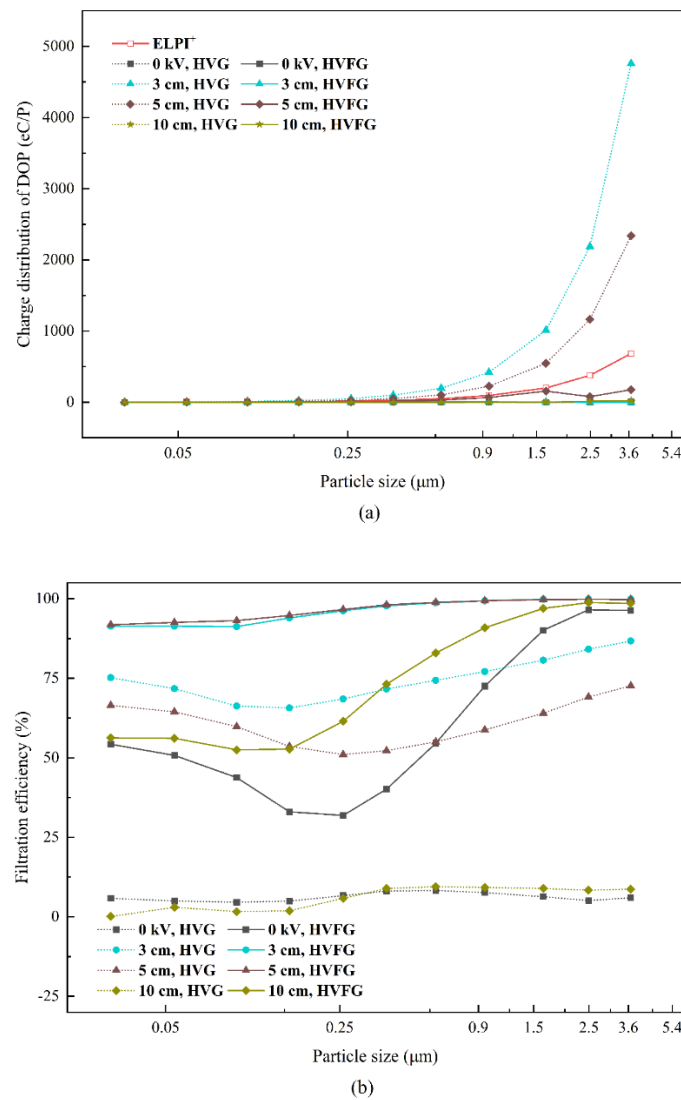
Figure 6. Effects of the electric field intensity on the DOP charging and filtration efficiency of coupled systems. (**a**) Charge distribution of DOP. (**b**) Filtration efficiency of the grounding system.

When the charging of DOP particles by the applied high negative DC voltage reaches or exceeds the stable charge of the ELPI[+] for aerosol charging, the filtration efficiency of the HVFG improves appreciably. This is because the measurement principle of the ELPI[+] is the conversion of the current obtained from the amply charged aerosol. When the average charge obtained by applying a voltage to the DOP aerosol is higher than that of the equipment, it is considered that the particles are amply charged. The charged aerosol particles move toward the grounding electrode under the effect of the electric field. In addition to interception, gravitational, inertial deposition, diffusion, and other mechanical effects, the filter material in the electric field has an electrostatic adsorption effect on particles through the existence of the Coulomb force. The increase in the aerosol charge is beneficial for filter material capturing particulate matter, such that the electrostatically enhanced fibrous filter system has higher filtration efficiency. Thus, with a further strengthening of the electric field, the increase in the DOP aerosol charge slows, and the improvement in the filtration efficiency of the coupled system slows, yet the efficiency remains high. If the electric field continues to strengthen, the electric field generated by the charge of aerosol particles gradually strengthens and generates a reverse Coulomb force. Therefore, the interaction between aerosol particles and free electrons for continual charging weakens,

which is unfavorable for rapidly increasing the DOP average charge, and the improvement of the filtration efficiency of the coupled system is thus limited.

Relatively speaking, for a particle size of 0.15–0.25 µm, the particle charging weakens the phenomenon of a permeable particle size in the coupled system, such that the improvement in the classification filtration efficiency of the original permeable particle size is most obvious. Aerosols smaller than 0.15 µm are mainly subject to a diffusion charge in the electric field, and the particle charge comes from the random diffusion of charged particles. A smaller aerosol particle is more easily able to pass through the diffusion charge. Aerosol particles larger than 0.5 µm are mainly affected by collision charge, and charged particles collide with other particles through the action of the electric field force to change the latter's charge. The charge is proportional to the quadratic power of the particle size. A larger particle is more easily charged by collision. Particles of size between 0.15 and 0.5 µm are affected by the two charging mechanisms and have relatively little charge, and they are not easily trapped by the electric field [30].

In the case of the filter material, particles smaller than 0.1 µm are captured under the diffusion effect, whereas particles larger than 0.4 µm are captured by mechanisms such as interception and inertial deposition, whereas for particles within the size range of 0.1–0.4 µm, the effect of the above mechanism is limited. Therefore, aerosol particles in the size range of 0.1–0.4 µm are the most penetrating and result in the poor effectiveness of the filter material, and the filtration efficiency is readily at a minimum in this particle size range [43]. The amply charged aerosol interacts with the filter material through the electrostatic force to greatly improve the filtration effect in this size range. In the present experiment, when the separation of the wire electrode and grounding electrode was 5 cm and a high voltage of 20 kV was applied, the filtration efficiency for a particle size of 0.25 µm in the coupled system increased to 96.6% from 31.8% for the filter material alone and to 51% for the electric field alone.

Figure 6b presents the filtration efficiency of the coupled system, showing that, compared with the DOP charge amount upstream and downstream of the HVFG, the original charge amount of DOP was low without an applied voltage and hardly changed after the DOP passed through the coupled system. When a high negative DC voltage was applied, the fully charged DOP particles were filtered by the coupled system, and the charge was reduced, indicating that the filter material better trapped the charged particles.

Figure 7 shows the effect of varying the electric field intensity by adjusting the voltage while fixing the electrode separation at 5 cm on the filtration efficiency of the HVFG. Figure 7a shows that the charge of DOP aerosol gradually increased with a strengthening electric field. At an applied voltage lower than −15 kV, the charge of the aerosol hardly changed and did not reach the ample charge of ELPI$^+$ for DOP charging. At an applied voltage of −20 kV, the charging of the aerosol by the coupled system was higher and exceeded the charge of the ample charge of ELPI$^+$ for DOP charging. Additionally, the results of the filtration efficiency of the coupled system in Figure 7b show that in the HVG, at an applied voltage of the electric field of −10 or −15 kV, the filtration efficiency did not improve. At an applied voltage of −20 kV, the filtration efficiency was approximately 25% higher than that at an applied voltage of −15 kV. In the electrostatically enhanced fibrous filter system, the improvement of the filtration efficiency was appreciable. At an applied voltage of −10 kV and a particle size of 0.25 µm, the filtration efficiency of the HVG was 28.5% and the filtration efficiency of the filter material was 30.5%, whereas the filtration efficiency of the HVFG was 94.6%. At an applied voltage of −20 kV, the filtration efficiency was 96.6%, and the charge of amply charged DOP after filtering by the filter material was reduced.

(a)

(b)
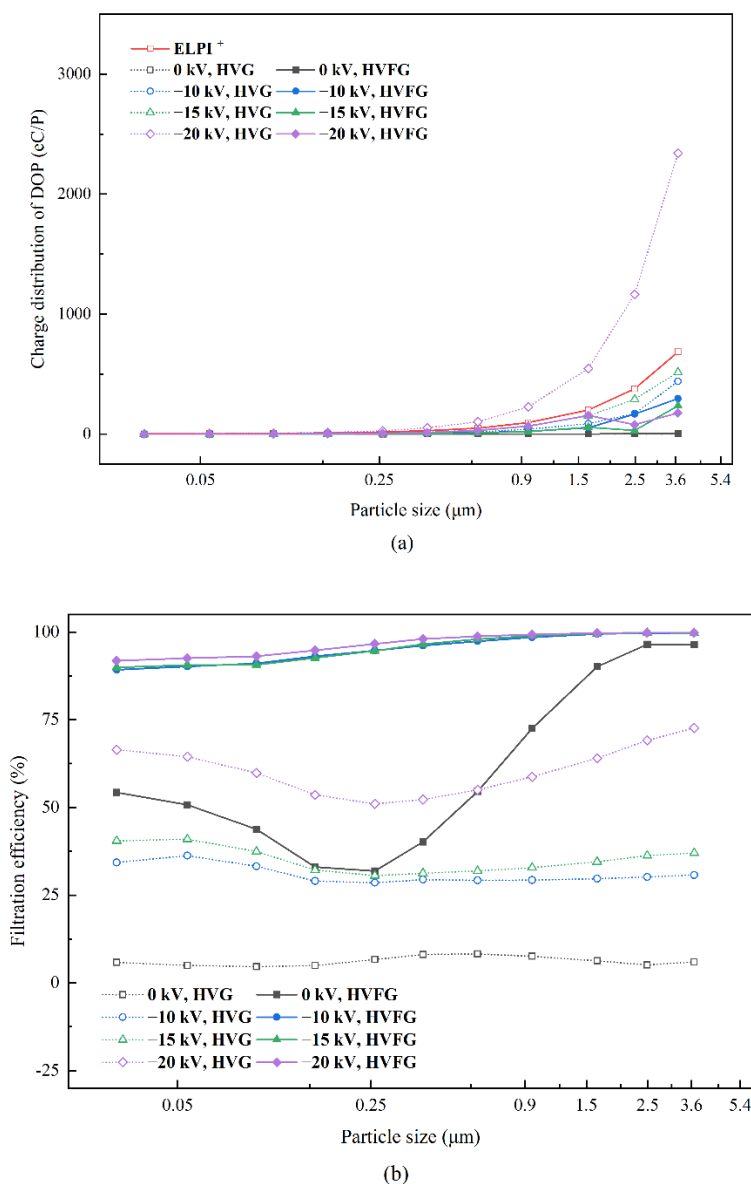
Figure 7. Effects of the electric field intensity on the DOP charging and filtration efficiency of coupled systems. (**a**) Charge distribution of DOP. (**b**) Filtration efficiency of the grounding system.

3.4. Effect of Coupled Systems on the Filtration Efficiency and Stability of the Filter Material

An electret filter material has the advantages of low flow resistance and high efficiency due to a special electrostatic effect originating from the polarization or charge of the fiber. However, the deposition of oily particles can cause the fast decay of electret charge in the filtering of oily aerosol, resulting in a rapid decline in filtration efficiency. To investigate the probability that the oil aerosol reduces the electret effect of the filter material when the aerosol covers the surface of the fiber in the coupled system, we studied the change in the filtration performance of the HVFG under the condition of continuously generating DOP aerosol for an experimental period of 1 h. For particles smaller than 1.5 μm, Figure 8a shows that the filtration efficiency of HVFG at 0 kV was stable at a low level for the period of 1 h. Figure 8b shows that the long-term filtration effect of the deposition of DOP aerosol in the coupled system was limited. For 0.25 μm particles, the filtration efficiency of the coupled system increased from 32.8% for the fiber acting alone to 96.2%. After continuous filtration for 60 min, the filtration efficiency of the coupled system slightly increased and remained at 99.1%. With an increase in the DOP particle size, the fractional efficiency increased slowly, and when the aerosol particles were larger than 0.29 μm, the filtration

efficiency of the coupled system remained above 99.5%. Additionally, for a small DOP particle size of 0.22 μm, when we turned off the external electric field after 1 h, the filtration efficiency of the fiber reached 79.6%, which was much higher than the initial filtration efficiency of the fiber acting alone (34.8%). This indicates that in the filtration process of the coupled system, not only was the aerosol charged but also the electret performance of the electret fiber improved.
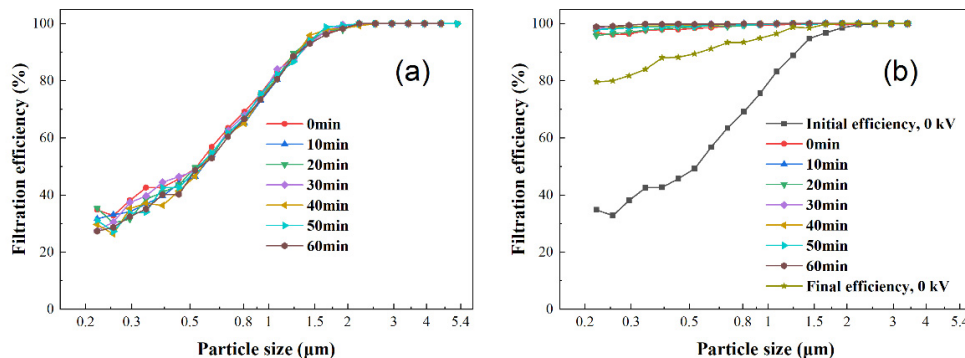
Figure 8. Filtration efficiency of the HVFG for a period of 1 h. (**a**) The HVFG at 0 kV (**b**) The HVFG at −25 kV.

In this experiment, an O_3 detector was used to monitor the O_3 generated during the filtration process of the coupled system. Figure 9 presents the concentration of O_3 for the HVFG with a more obvious coupling effect. By adjusting the separation of the wire electrode and grounding electrode to vary the electric field intensity, it was found that the quantity of generated O_3 depended on the electric field. Figure 9 shows that when the distance of the wire electrode and grounding electrode was 1, 3, 5, and 10 cm, the peak concentration of O_3 was 6.3, 24.3, 36.5, and 26.3 ppb, respectively, which meets indoor O_3 concentration standards.
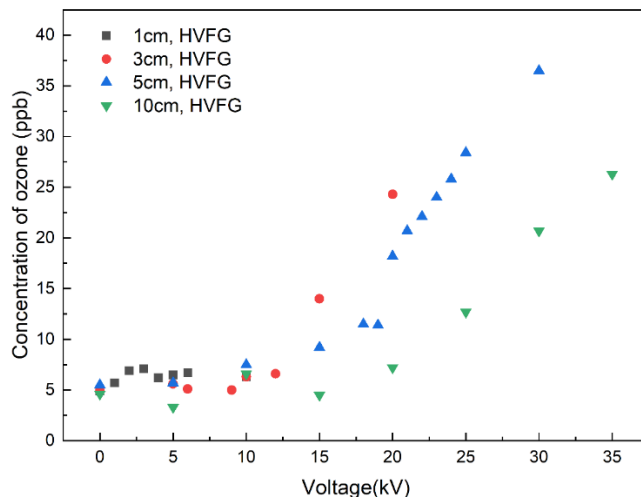
Figure 9. Concentration of O_3 for the HVFG.

4. Conclusions

The following conclusions are drawn from the results of the study:

(1) In the electrostatically enhanced fibrous filter system, the charge of the aerosol is the main factor affecting the coupling effect. Increasing the charge of the aerosol improves the DOP filtration efficiency of the coupled system. Both the form of coupling and the strength of the electric field affect the charge of DOP aerosol. The arrangement of an electric field with a grounding electrode is more conducive to the charging of aerosol and has a better effect on filtration;

(2) For the filter media or electric field, the DOP aerosol has a permeable particle size range of 0.15–0.25 μm. In the electrostatically enhanced fibrous filter system, there is no longer the phenomenon of the most permeable particle size because the charge of the aerosol and filter media increases the Coulomb force in the filtration process. The filtration efficiency gradually increases with the enlargement of particles, reaching 96.6% at a particle size of 0.25 μm;

(3) The electrostatically enhanced fibrous filter system restores the filtration efficiency of electret materials and effectively enhances the long-term stability of electret materials in filtering oily aerosol.

Author Contributions: Conceptualization, S.-P.B., H.H., H.S. and J.K.; methodology, Y.Y., D.P., K.K., S.-P.B., H.H., H.S. and J.K.; validation, Y.Y., H.H. and H.S.; investigation, Y.Y., D.P. and H.S.; resources, K.K., S.-P.B. and J.K.; data curation, Y.Y., D.P. and H.S.; writing—original draft preparation, Y.Y., D.P. and K.K.; writing—review and editing, S.-P.B., H.H., H.S. and J.K.; supervision, H.S. and J.K.; project administration, S.-P.B., H.S. and J.K. All authors have read and agreed to the published version of the manuscript.

References

1. Huang, R.; Zhang, Y.; Bozzetti, C. High secondary aerosol contribution to particulate pollution during haze events in China. *Nature* **2014**, *514*, 218–222. [CrossRef] [PubMed]
2. Amaral, S.S.; de Carvalho, J.A., Jr.; Costa MA, M.; Pinheiro, C. An Overview of Particulate Matter Measurement Instruments. *Atmosphere* **2015**, *6*, 1327–1345. [CrossRef]
3. Liu, X.; Wang, S.; Zhang, Q.; Jiang, C.; Liang, L.; Tang, S.; Zhang, X.; Han, X.; Zhu, L. Origins of black carbon from anthropogenic emissions and open biomass burning transported to Xishuangbanna, Southwest China. *J. Environ. Sci.* **2023**, *125*, 277–289. [CrossRef]
4. Zhang, C.; Zhang, Y.; Liu, X.; Liu, Y.; Li, C. Characteristics and source apportionment of PM2. 5 under the dual influence of the Spring Festival and the COVID-19 pandemic in Yuncheng city. *J. Environ. Sci.* **2023**, *125*, 553–567. [CrossRef]
5. Gao, J.; Chao, H.; Li, T. Advancements in technologies for improving dust removal effectiveness of electrostatic precipitators. *Environ. Pollut. Control* **2007**, *29*, 763–766.
6. Zhang, H.; Liu, N.; Zeng, Q.; Liu, J.; Zhang, X.; Ge, M.; Zhang, W.; Li, S.; Fu, Y.; Zhang, Y. Design of polypropylene electret melt blown nonwovens with superior filtration efficiency stability through thermally stimulated charging. *Polymers* **2020**, *12*, 2341. [CrossRef]
7. Afshari, A.; Ekberg, L.; Forejt, L.; Mo, J.; Rahimi, S.; Siegel, J.; Chen, W.; Wargocki, P.; Zurami, S.; Zhang, J. Electrostatic Precipitators as an Indoor Air Cleaner—A Literature Review. *Sustainability* **2020**, *12*, 8774. [CrossRef]
8. Kanaoka, C. Fine Particle Filtration Technology Using Fiber as Dust Collection Medium. *KONA Powder Part. J.* **2019**, *36*, 88–113. [CrossRef]
9. Abdolghader, P.; Brochot, C.; Haghighat, F.; Bahloul, A. Airborne nanoparticles filtration performance of fibrous media: A review. *Sci. Technol. Built Environ.* **2018**, *24*, 648–672. [CrossRef]
10. Liu, C.; Dai, Z.; He, B.; Ke, Q.F. The Effect of Temperature and Humidity on the Filtration Performance of Electret Melt-Blown Nonwovens. *Materials* **2020**, *13*, 4774. [CrossRef]
11. Jaworek, A.; Sobczyk, A.T.; Krupa, A.; Marchewicz, A.; Czech, T.; Śliwiński, L. Hybrid electrostatic filtration systems for fly ash particles emission control. A review. *Sep. Purif. Technol.* **2019**, *213*, 283–302. [CrossRef]
12. Stenhouse, J. Clogging of an electrically active fibrous filter material: Experimental results and two-dimensional simulations. *Powder Technol.* **1997**, *93*, 63–75.
13. Huang, B.; Yao, Q.; Li, S.Q.; Zhao, H.L.; Song, Q.; You, C.F. Experimental investigation on the particle capture by a single fiber using microscopic image technique. *Powder Technol.* **2006**, *163*, 125–133. [CrossRef]
14. Bugarski, A.D.; Hummer, J.A. Contribution of various types and categories of diesel-powered vehicles to aerosols in an underground mine. *J. Occup. Environ. Hyg.* **2020**, *17*, 121–134. [CrossRef]
15. Oeder, S.; Kanashova, T.; Sippula, O.; Sapcariu, S.C.; Streibel, T.; Arteaga-Salas, J.M.; Passig, J.; Dilger, M.; Paur, H.-R.; Schlager, C.; et al. Particulate matter from both heavy fuel oil and diesel fuel shipping emissions show strong biological effects on human lung cells at realistic and comparable in vitro exposure conditions. *PLoS ONE* **2015**, *10*, e0126536.

16. Dasch, J.; D'Arcy, J.; Gundrum, A.; Sutherland, J.; Johnson, J.; Carlson, D. Characterization of fine particles from machining in automotive plants. *J. Occup. Environ. Hyg.* **2005**, *2*, 609–625. [CrossRef]
17. Sheng, Y.; Zhang, L.; Wang, Y.; Miao, Z. Exploration of a novel three-dimensional knitted spacer air filter with low pressure drop on cooking fume particles removal. *Build. Environ.* **2020**, *177*, 106903. [CrossRef]
18. Guo, C.; Gao, Z.; Shen, J. Emission rates of indoor ozone emission devices: A literature review. *Build. Environ.* **2019**, *158*, 302–318. [CrossRef]
19. Boelter, K.J.; Davidson, J.H. Ozone generation by indoor, electrostatic air cleaners. *Aerosol Sci. Technol.* **1997**, *27*, 689–708. [CrossRef]
20. Waring, M.S.; Siegel, J.A.; Corsi, R.L. Ultrafine particle removal and generation by portable air cleaners. *Atmos. Environ.* **2008**, *42*, 5003–5014. [CrossRef]
21. De Oliveira, A.E.; Guerra, V.G. Electrostatic precipitation of nanoparticles and submicron particles: Review of technological strategies. *Process Saf. Environ. Prot.* **2021**, *153*, 422–438. [CrossRef]
22. Tu, G.; Song, Q.; Chen, K.; Yao, Q. Study on the Charge Decay of Charged Particles During Particle Transportation. *Proc. Csee* **2016**, *36*, 4369–4375.
23. Gao, Y.; Tian, E.; Zhang, Y.; Mo, J. Utilizing electrostatic effect in fibrous filters for efficient airborne particles removal: Principles, fabrication, and material properties. *Appl. Mater. Today* **2022**, *26*, 1369. [CrossRef]
24. Chen, K.; Huang, Y.; Wang, S.; Zhu, Z.; Lou, T.; Cheng, H. Experimental study on graded capture performance of fine particles with electrostatic-fabric integrated precipitator. *Powder Technol.* **2022**, *402*, 117297. [CrossRef]
25. Stepkina, M.Y.; Kudryashova, O.B.; Antonnikova, A. Sedimentation of a Fine Aerosol in the Acoustic Field and with the Electrostatic Charge of Particles. *Arch. Acoust.* **2018**, *43*, 69–73.
26. Tang, M.; Junbin, Y.U.; Ling, H.E.; Wang, L.; Wang, T. The Accumulation Mechanism of Charged Particles on the Surface of Bag Filter in EBP. *Ind. Saf. Environ. Prot.* **2015**, *41*, 79–83.
27. Feng, Z.; Long, Z.; Mo, J. Experimental and theoretical study of a novel electrostatic enhanced air filter (EEAF) for fine particles. *J. Aerosol Sci.* **2016**, *102*, 41–54. [CrossRef]
28. Feng, Z.; Long, Z.; Yu, T. Filtration characteristics of fibrous filter following an electrostatic precipitator. *J. Electrost.* **2016**, *83*, 52–62. [CrossRef]
29. Xu, Y.; Zheng, C.; Liu, Z.; Yan, K. Electrostatic precipitation of airborne bio-aerosols. *J. Electrost.* **2013**, *71*, 204–207. [CrossRef]
30. Jianan, W.; Xue, W.; Tingyu, Z.; Yi, Z. Experimental study on the impact of electrostatic effect on the movement of charged particles. *J. Electrost.* **2018**, *94*, 14–20. [CrossRef]
31. Donovan, R.P.; Hovis, L.S.; Ramsey, G.H.; Ensor, D.S. Electric-Field-Enhanced Fabric Filtration of Electrically Charged Flyash. *Aerosol Sci. Technol.* **1982**, *1*, 385–399. [CrossRef]
32. Luckner, J.; Wertejuk, Z.; Gradoń, L. Experimental studies of the fibrous filters coupled with external electrical field. *J. Aerosol Sci.* **1995**, *26*, S915–S916. [CrossRef]
33. Luckner, H.; Gradoń, L.; Podgórski, A.; Wertejuk, Z. Separation of liquid aerosol particles in cyclones and fibrous filters conjugated with external electric field. *J. Aerosol Sci.* **1999**, *30*, 743–744. [CrossRef]
34. Tarasenko, V.F.; Baksht, E.K.; Vinogradov, N.P.; Kozyrev, A.V.; Kokovin, A.S.; Kozhevnikov, V.Y. On the Mechanism of Generation of Trichel Pulses in Atmospheric Air. *JETP Lett.* **2022**, *115*, 667–672. [CrossRef]
35. Berendt, A.; Budnarowska, M.; Mizeraczyk, J. DC negative corona discharge characteristics in air flowing transversely and longitudinally through a needle-plate electrode gap. *J. Electrost.* **2018**, *92*, 24–30. [CrossRef]
36. Ouyang, J.; Zhang, Z.; Zhang, Y.; Peng, Z.L. Experimental Study on the Characteristics of Negative-corona Trichel Pulses in Air. *High Volt. Eng.* **2014**, *40*, 1194–1200.
37. Sattari, P.; Gallo, C.F.; Castle GS, P.; Adamiak, K. Trichel pulse characteristics—Negative corona discharge in air. *J. Phys. D Appl. Phys.* **2011**, *44*, 155502. [CrossRef]
38. Guo, Y.; Zhang, X.; Li, Y.; Zhang, G.; Sun, A. Effect of transverse airflow on the deflection of negative corona discharge on the Trichel pulse mode at atmospheric pressure. *AIP Adv.* **2021**, *11*, 125107. [CrossRef]
39. Lu, B.X.; Song, L.J. The study of negative needle-to-plane corona discharge with photoionization under various air pressures. *AIP Adv.* **2021**, *11*, 085013. [CrossRef]
40. INTRA, P. Corona discharge in a cylindrical triode charger for unipolar diffusion aerosol charging. *J. Electrost.* **2012**, *70*, 136–143. [CrossRef]
41. Alguacil, F.J.; Alonso, M. Multiple charging of ultrafine particles in a corona charger. *J. Aerosol Sci.* **2006**, *37*, 875–884. [CrossRef]
42. Hernandez-Sierra, A.; Alguacil, F.J.; Alonso, M. Unipolar charging of nanometer aerosol particles in a corona ionizer. *J. Aerosol Sci.* **2003**, *34*, 733–745. [CrossRef]
43. Bortolassi, A.C.C.; Nagarajan, S.; de Araújo Lima, B.; Guerra, V.G.; Aguiar, M.L.; Huon, V.; Soussan, L.; Cornu, D.; Miele, P.; Bechelany, M. Efficient nanoparticles removal and bactericidal action of electrospun nanofibers membranes for air filtration. *Mater. Sci. Eng. C* **2019**, *102*, 718–729. [CrossRef] [PubMed]